

Research Article

A Kinetic Study of Marginal Soil Energy Plant *Helianthus annuus* Stalk Pyrolysis

Huaxiao Yan,^{1,2} Hui Zhao,^{1,2} Yan Zhang,^{1,2} Yuanyu Tian,^{1,2} and Kechang Xie²

¹ College of Chemical and Environmental Engineering, Shandong University of Science and Technology, Qingdao 266590, China

² Key Laboratory of Low-carbon Energy Chemical Engineering in Universities of Shandong, Shandong University of Science and Technology, Qingdao 266590, China

Correspondence should be addressed to Hui Zhao; zhsdust@126.com

Received 17 December 2012; Accepted 21 January 2013

Academic Editor: Xiumin Jiang

Copyright © 2013 Huaxiao Yan et al. This is an open access article distributed under the Creative Commons Attribution License, which permits unrestricted use, distribution, and reproduction in any medium, provided the original work is properly cited.

The pyrolytic characteristics and kinetics of new marginal soil energy plant *Helianthus annuus* stalk were investigated using thermogravimetric (TG) method from 50 to 800°C in an inert argon atmosphere at different heating rates of 5, 10, 20 and 30°C min⁻¹. The kinetic parameters of activation energy and pre-exponential factor were deduced by Popescu, Flynn-Wall-Ozawa (FWO), and Kissinger-Akahira-Sunose (KAS) methods, respectively. The results showed that three stages appeared in the thermal degradation process. The primary devolatilization stage of *H. annuus* stalk can be described by the Avrami-Erofeev function ($n = 4$). The average activation energy of *H. annuus* stalk was only 142.9 kJ mol⁻¹. There were minor kinetic compensation effects between the pre-exponential factor and the activation energy. The results suggest that *H. annuus* stalk is suitable for pyrolysis, and more importantly, the experimental results and kinetic parameters provided useful information for the design of pyrolytic processing system using *H. annuus* stalk as feedstock.

1. Introduction

As potential “next generation” biofuel feedstock, marginal soil plants have attracted considerable attention because of their advantages, such as high photosynthetic efficiency, maximum biomass production, fast growing, high conversion rate, ease of harvesting, and lack of arable soil requirements. *Helianthus annuus* can grow well in barren marginal lands and has good resistance to adverse situations. Moreover, it does not compete with grain crops for arable lands, which is significant for one populous country lack of arable land as China. The agriculture is producing huge amount of *H. annuus* stalks as by-products of seeds every year in China. It has been reported that the stalk yield was ranging between 5 and 14 tons per hectare. *H. annuus* has an excellent adaptability, and the growth cycle is only about 100 days. These characteristics of *H. annuus* suggest that it can be used as a good potential energy source and should be further studied as a good biofuel feedstock candidate [1–8].

Biomass pyrolysis has demonstrated itself to be a kind of biomass-energy utilization technology which transforms

low-energy density biomass materials into high-energy density liquid products which can be utilized more efficiently in an environment-friendly manner. A thorough knowledge of the thermal behavior and pyrolysis kinetics of biomass are required for the proper design and operation of the pyrolysis conversion systems. Thermogravimetry (TG) analysis method was selected to investigate the thermal decomposition process. The kinetic data from TG are not only very useful for understanding the thermal degradation processes and mechanisms, but also can be used as input parameters for a thermal degradation reaction system [9–11].

In present study, *H. annuus* stalk pyrolysis was investigated using a TG/DSC instrument with nonisothermal thermogravimetric (TG) analysis method at different heating rates under an inert atmosphere. The pyrolysis characteristics and kinetics were examined by Popescu, Flynn-Wall-Ozawa (FWO) and Kissinger-Akahira-Sunose (KAS) methods and then the average activation energy, pre-exponential factors, and reaction orders were deduced. The objective of this study was to obtain the kinetic parameters of thermal decomposition and then to determine the degradation mechanism for

facilitating the efficient design, operation, and modeling of pyrolysis and related thermochemical conversion systems for energy plants.

2. Materials and Methods

2.1. Materials. *H. annuus* stalk was collected from the marginal land of Shandong University of Science and Technology campus, Qingdao, China, January 2012. Sample was dried in one drying oven at $100 \pm 2^\circ\text{C}$ for 10 hours and pulverized in a plant disintegrator to be able to pass through a 120-mesh sieve, and then stored in a desiccator.

2.2. Proximate and Component Analysis of the Sample. Proximate analysis was carried out according to the national standard GB212-91 (China). For analysis of composition, the biomass materials were hydrolyzed using 72% H_2SO_4 , 2 mol/L HCl and concentrated HCl to analyze cellulose, hemicellulose and lignin contents according to established methods, respectively [10, 12, 13]. The results were presented in Table 1. All tests were carried out in triplicate.

2.3. Pyrolysis by Thermogravimetric Analyzer. Pyrolytic characteristics were determined by using a thermal analyzer (TGA/DSC1/1600LF Mettler Toledo Co., Switzerland). In the experiment, argon gas was used as a carrier gas with a flow rate of $50 \text{ cm}^3 \text{ min}^{-1}$. The heating rate was controlled at 5, 10, 20, $30^\circ\text{C min}^{-1}$ from 50 to 800°C . The sample mass that was used for the thermogravimetric analysis in each experiment was 10 mg approximately. Mass loss and calorific changes in response to temperature were recorded and used to plot thermogravimetric (TG), derivative thermogravimetric analysis (DTG), and differential scanning calorimetric (DSC) curves [14, 15]. All experiments were replicated three times. The software Origin 8.0 was used to analyze the data and plot the curves.

2.4. Kinetic Analysis

2.4.1. Popescu Method. The Popescu method was used to evaluate the most probable mechanism of the pyrolytic reaction [12, 13]. In other words, the Arrhenius equation was selected to analyze the thermal decomposition reactions. The dynamic equation is:

$$\frac{d\alpha}{dt} = k(T) f(\alpha), \quad (1)$$

where α is the conversion rate and is defined as follows:

$$\alpha = \frac{m_0 - m}{m_0 - m_\infty} \quad (2)$$

and here, m_0 , m , m_∞ are the initial, actual, and the end mass of samples, mg;

where $k(T)$ is the velocity constant, and $f(\alpha)$ is the differential coefficient mechanism function.

Consider

$$k(T) = A \exp\left(-\frac{E}{RT}\right) \quad (3)$$

TABLE 1: Proximate and component analysis of *H. annuus* stalk.

Characteristics	<i>H. annuus</i> stalk
Proximate analysis ^a /wt%	
Moisture (M_{ar})	9.93 ± 0.46
Ash (A_{ar})	4.08 ± 0.01
Volatile matter (V_{ar})	72.94 ± 0.42
Fixed carbon ^b (FC_{ar})	13.05
Component analysis/wt%	
Cellulose	21.13 ± 1.19
Hemicellulose	14.81 ± 0.37
Lignin	7.30 ± 1.52

^a Mass percentage on as-received basis; ^b calculated by difference.

thus, with the combination of (1), (2), and (3), the rate of a solid-state reaction can generally be described by:

$$\frac{d\alpha}{dt} = A \exp\left(-\frac{E}{RT}\right) f(\alpha) \quad (4)$$

and then, if the temperature is controlled at a constant heating rate, $\beta(\text{K/min}) = dT/dt$. Therefore, (4) gives:

$$\frac{d\alpha}{dT} = \frac{1}{\beta} k(T) f(\alpha) = \frac{A}{\beta} \exp\left(-\frac{E}{RT}\right) f(\alpha). \quad (5)$$

Then the integral form of (5) is:

$$\begin{aligned} G(\alpha)_{mn} &= \int_{\alpha_m}^{\alpha_n} \frac{d\alpha}{f(\alpha)} = \frac{1}{\beta} \int_{T_m}^{T_n} k(T) dT = \frac{1}{\beta} I(T)_{mn} \\ &= \frac{A}{\beta} H(T)_{mn}. \end{aligned} \quad (6)$$

For this equation, where α_m , α_n are two different degrees of conversion, and T_m , T_n are their corresponding temperatures, and here $I(T)_{mn}$, $H(T)_{mn}$ and $T\delta$ can be described as follows, respectively:

$$I(T)_{mn} = \int_{T_m}^{T_n} k(T) dT,$$

$$H(T)_{mn} = \int_{T_m}^{T_n} \exp\left(-\frac{E}{RT}\right) = (T_n - T_m) \exp\left(-\frac{E}{RT\delta}\right), \quad (7)$$

$$T\delta = \frac{T_m + T_n}{2}.$$

Therefore, a plot of $G(\alpha)_{mn}$ versus $1/\beta_i$ gives a straight line with an intercept of zero. If the experiment data and $G(\alpha)_{mn}$ are chosen properly, a plot of $G(\alpha)_{mn}$ versus $1/\beta_i$ gives a straight line with an intercept of zero. Then, this $G(\alpha)_{mn}$ is the proper mechanism that can express the true chemical reaction process.

By logarithmic transformation of (6), a linear equation is deduced:

$$\ln\left(\frac{\beta}{T_n - T_m}\right) = \ln\left[\frac{A}{G(\alpha)}\right] - \frac{E}{RT\delta}. \quad (8)$$

A plot of $\ln(\beta/(T_n - T_m))$ versus $1/T\delta$ gives a straight line with a slope of $-E/R$ and intercept of $\ln[A/G(\alpha)]$. Therefore, E and $\ln A$ can be determined.

TABLE 2: Temperature characteristics associated with the pyrolysis process of *H. annuus* stalk.

Heating rate/ $^{\circ}\text{C min}^{-1}$	Temperature/ $^{\circ}\text{C}$				
	T_1	T_2	T_3	T_4	T_5
5	196.3	259.2	296.7	322.9	365.4
10	151.7	216.0	260.0	284.6	342.1
20	130.4	183.4	209.0	231.7	272.5
30	161.3	244.2	261.3	296.3	330.4

2.4.2. *FWO and KAS Method.* It is well known that flynn-wall-ozawa (FWO) method and kissinger-akahira-sunose (KAS) method were generally used to deduce the activation energy and pre-exponential factor, and the apparent activation energy is influenced by temperature T and fractional conversion α [13, 16–20]. So, activation energy can be obtained with the change of heating rate β .

Flynn-Wall-Ozawa equation:

$$\ln \beta = \ln \left[\frac{0.0048AE}{RG(\alpha)} \right] - 1.0516 \frac{E}{RT}. \quad (9)$$

KAS equation:

$$\ln \left(\frac{\beta}{T^2} \right) = \ln \left[\frac{AR}{EG(\alpha)} \right] - \frac{E}{RT}. \quad (10)$$

According to (9) and (10), plots of $\ln \beta$, $\ln(\beta/T^2)$ versus $1/T$ with a certain conversion rate α give straight lines with slopes of $-1.0516E/RT$, and $-E/R$ the activation energy can be determined. Then, the activation energy (E) can be determined. Substituting the value of E and the mechanism function $G(\alpha)$ back into (9) and (10) in conjunction with T and α , $\ln A$ can be calculated.

3. Results and Discussion

3.1. *Characteristics of the Thermal Degradation Process.* According to thermogravimetric (TG) and differential thermogravimetric (DTG) curves of *H. annuus* stalk (Figures 1 and 2), the results indicated that the pyrolysis process was made up of three stages. The stage I occurred as the temperature increased from room temperature to T_1 , while the second started as the temperature that increased from T_1 to T_5 (II). However, the sample revealed somewhat different during stage II. Stage II included two zones for *H. annuus* stalk pyrolysis process: zone I occurred as the temperature increased from T_1 to T_3 with a maximum mass loss point at T_2 , and zone II occurred as the temperature increased from T_3 to T_5 with a maximum mass loss point at T_4 . The last one, stage III occurred as the temperature increased from T_5 to 800°C . The concrete contents of the temperature characteristics were shown in Table 2 and Figure 2.

The TG and DTG curves of the sample at different heating rates (Table 2) and $20^{\circ}\text{C min}^{-1}$ (Figures 1 and 2, all profiles of different heating rates are not presented here, and $20^{\circ}\text{C min}^{-1}$ was shown as an example for concision) showed that three stages appeared corresponding to three different pyrolytic

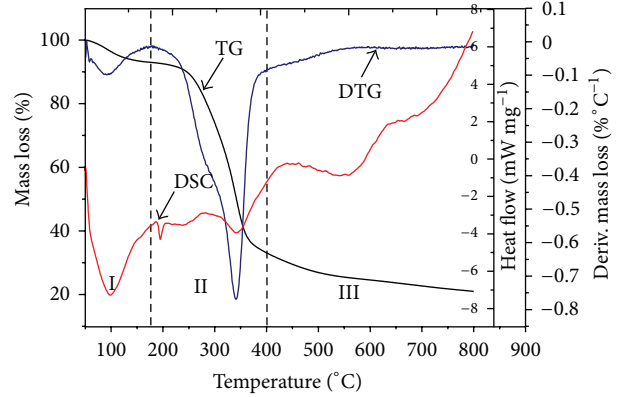


FIGURE 1: TG-DTG-DSC curves of *H. annuus* stalk at the heating rate of $20^{\circ}\text{C min}^{-1}$ (as an example for concision).

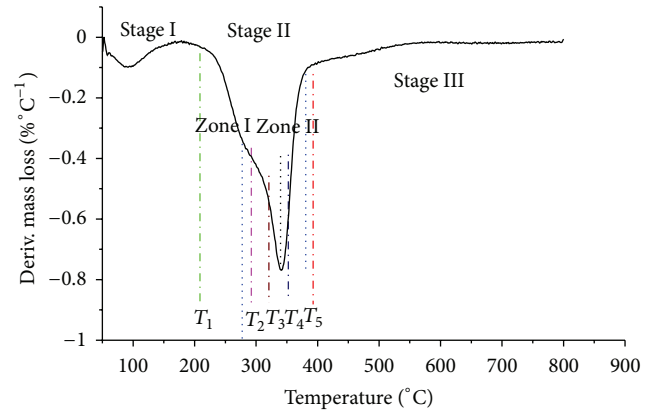


FIGURE 2: The DTG curves of *H. annuus* stalk at the different heating rate of $20^{\circ}\text{C min}^{-1}$ with the characteristic temperature zone.

processes. The stage I was the process of slow mass loss corresponding to the evaporation of water and other volatile components, in other words, it is that both the internal cellular water and the external water bound by surface tension were lost [12]. From the Figure 2, stage II (T_1 – T_5) was the devolatilization stage, during which the main pyrolytic process occurred. In this stage, various volatile components were gradually released, and biological macromolecules were depolymerized and fractured; that resulted in a large mass loss and formation of the main pyrolytic products. The temperature range of three samples during stage II was 130.4 – 272.5°C (*H. annuus* stalk) at different heating rates. During the stage III, the residual was slowly decomposed [26], resulting in the formation of a loose porous end-product.

Heating rates have significant effects on the pyrolysis process. As the heating rate increasing, the mass loss rate and the average reaction rate both increased. The results were shown in Table 3.

The differential scanning calorimetry (DSC) curves of three samples at different heating rates were presented in

TABLE 3: Mass loss and average reaction rate at different stages of *H. annuus* stalk pyrolysis process.

Stage			Heating rate/ $^{\circ}\text{C min}^{-1}$			
			5	10	20	30
I	ML ^a		6.6	7.1	7.0	6.5
	AR ^b		0.2	0.6	1.1	1.5
II	Z I ^c	ML ^a	23.3	23.2	21.0	18.1
		AR ^b	1.2	1.8	3.3	4.5
	Z II ^d	ML ^a	32.9	36.8	39.3	39.2
		AR ^b	2.4	3.7	7.8	14.2
III	ML ^a		16.1	13.3	11.6	13.0
	AR ^b		0.2	0.3	0.6	0.9
Final residual at 800 $^{\circ}\text{C}$ ^e			21.1	19.6	21.0	23.2

^a Mass loss, %; ^b Average reaction rate, %/min; ^c Zone I; ^d Zone II; ^e Final residual at 800 $^{\circ}\text{C}$, %.

TABLE 4: The linear fitting results of kinetic mechanism functions of *H. annuus* stalk.

Function	Temperature/ $^{\circ}\text{C}$	<i>R</i>	SD
$[-\ln(1 - \alpha)]^4$	200	0.96601	0.00145
Avrami-Erofeev	250	0.98151	0.01246
Function	300	0.99083	0.07635
$n = 4$	350	0.99305	0.13633

R: Correlation coefficient; SD: standard deviation.

Figure 3. As the heating rate increasing, an obvious exothermic effect appeared, and this finding indicated that the pyrolysis process produced heat. During the stage I, there was an obvious endothermic peak, which corresponded to moisture evaporation. In stage II (devolatilization stage), there were some differences among these three samples. As the temperature increased, *H. annuus* stalk maintained the exothermic effect, while as the heating rate increasing, the exothermic effect became more obvious with the peak area increased. At the temperature of 400 to 500 $^{\circ}\text{C}$, there was an exothermic peak, which showed that the charring process occurred at this moment. Generally speaking, an endothermic process can be related to depolymerization and volatilization processes, while an exothermic process is due to charring. The pyrolysis had no clear endothermic effects, which suggested that the decomposition process needs low energy and the inorganic salts promote charring and exothermic effects.

3.2. Kinetic Analysis of the Pyrolysis Process

3.2.1. Determination of $G(\alpha)$. Different conversion rates at different heating rates and temperatures were chosen to determine the pyrolysis mechanism function. These temperatures should be applied during stage II. The 41 kinds of typical mechanism functions [27] were analyzed according to the Popescu method to determine the $G(\alpha)$ function. And at last, according to these 41 kinds of typical mechanism functions, the function ($G(\alpha) = [-\ln(1 - \alpha)]^4$) appeared as the most probable mechanism function for *H. annuus* stalk (Table 4).

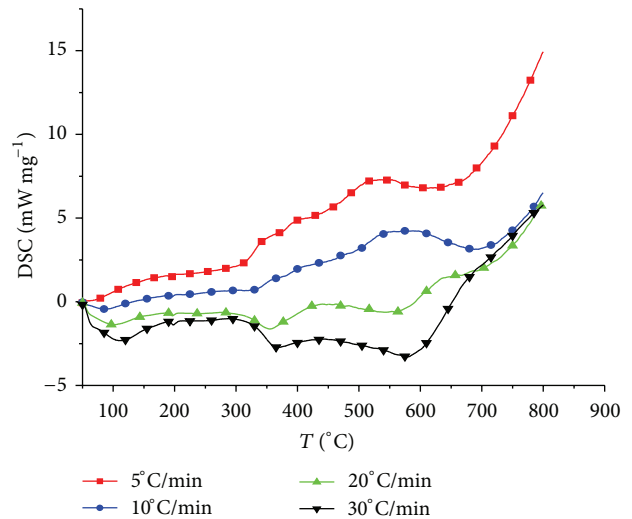


FIGURE 3: The DSC curves of *H. annuus* stalk at different heating rates.

And then, the activation energy and pre-exponential factors can be calculated by function $G(\alpha)$ [28].

3.2.2. Calculation of the Activation Energy and Pre-Exponential Factors. According to (8), a plot of $\ln(\beta/(T_n - T_m))$ versus $1/T\delta$ gives a straight line with a slope of $-E/R$ and intercept of $\ln[A/G(\alpha)]$. Therefore, E and $\ln A$ can be determined. And on basis of (9) and (10), a plot of $\ln \beta$, $\ln(\beta/T^2)$ against $1/T$ should be a linear relationship by FWO method and KAS method. Similarly, the activation energy and pre-exponential can be calculated (Figure 4). The values of activation energy and $\ln A$ was listed in Table 5. The value of R -Square was close to 0.9500, that is to say, the values of coefficient of correlation were relatively high. So the values of activation energy deduced and calculated by Popescu, FWO, and KAS methods are valid. However, the values of activation energy increased with a different fluctuation at different conversion rates. This

TABLE 5: The activation energies of *H. annuus* stalk obtained by FWO method and KAS method at different conversion rates.

Conversion rate/ α	FWO method			KAS method			Popescu method			
	$E/kJ Mol^{-1}$	R	$\ln A/min^{-1}$	$E/kJ Mol^{-1}$	R	$\ln A/min^{-1}$	Conversion Rate/ α	$E/kJ Mol^{-1}$	R	$\ln A/min^{-1}$
0.1	209.9	0.9997	20.70	214.7	0.9997	19.56	0.1–0.2	88.4	0.9091	12.83
0.2	178.5	0.9976	17.54	183.2	0.9977	16.72	0.2–0.3	115.5	0.9406	20.11
0.3	148.0	0.9849	15.48	152.4	0.9855	13.03	0.3–0.4	131.1	0.9463	24.28
0.4	128.9	0.9575	13.10	133.2	0.9590	11.73	0.4–0.5	138.1	0.9457	26.43
0.5	121.3	0.9190	12.02	125.5	0.9218	12.57	0.5–0.6	128.2	0.8957	25.14
0.6	128.2	0.8968	12.56	132.5	0.9006	11.39	0.6–0.7	119.4	0.8878	24.27
0.7	139.8	0.9067	13.55	144.2	0.9105	12.22	0.7–0.8	136.4	0.8271	28.66
0.8	142.0	0.9160	14.41	146.3	0.9195	9.04	0.8–0.9	195.0	0.9644	41.34
0.9	120.6	0.9043	10.81	124.6	0.9077	10.77				
Average	146.4 \pm 29.71			150.7 \pm 29.94			131.5 \pm 30.17			
Average	142.9 \pm 10.08									

E : Activation energy; A : pre-exponential factor; R : correlation coefficient.

TABLE 6: Comparison of various kinetic parameters of pyrolysis for different biomasses.

Sample	Decomposition temperature/ $^{\circ}C$	$E/kJ mol^{-1}$	References
<i>H. annuus</i> stalk	196.3–330.4	142.9	Present study
<i>Enteromorpha prolifera</i>	174–551	228.1	[21]
<i>Spirulian platensis</i>	190–560	42.2–5.25	[22]
Wheat straw	230–400	130–175	[23]
Sunflower shell	300–600	73.81	[24]
Rice husk	225–350	79.9	[25]

TABLE 7: Kinetic compensation effects of the pre-exponential factor and the activation energy.

Method	Equation	R
FWO method	$\ln A = 0.102E - 0.3927$	0.9654
KAS method	$\ln A = 0.095E - 1.3721$	0.7603
Popescu method	$\ln A = 0.263E - 9.2219$	0.9659

may be ascribed to the complex composition of the sample and the complex reactions during pyrolysis. In the end, the average activation energy value of *H. annuus* stalk was 142.9 $kJ mol^{-1}$.

In Table 6, various kinetic parameters of pyrolysis between different biomass sources were compared. Other results are not similar to the present study, which suggests that thermal behavior is influenced greatly by feedstock types [29].

In Table 7, the kinetic compensation effects of the pre-exponential factors and activation energy were shown. These results indicated that there was a partial compensation effect for A when E changed.

4. Conclusions

High priority should be given to the development and protection of biomass pyrolysis from new marginal soil energy

plant with great potential, which is widely recognized as a technically feasible way for sustainability. In the present work, there were three stages in the process of *H. annuus* stalk pyrolysis, and stage II was the main pyrolysis process, and most of the organic materials were decomposed in this stage, and heating rates had a significant effect on the pyrolysis process of biomass.

The Popescu, FWO, and KAS methods were adopted to determine the kinetic parameters of the pyrolysis reaction. During the primary decomposition reactions, the most probable mechanism functions for *H. annuus* stalk was $[-\ln(1-\alpha)]^4$. The values of activation energy calculated by these three methods were similar. There was only a partial compensation effect for A when E changed. The results suggest that *H. annuus* stalk is suitable for pyrolysis, and more importantly, the experimental results and kinetic parameters provided useful information for the design of pyrolytic processing system using *H. annuus* stalk as feedstock.

Conflict of Interests

The authors declare that they have no conflict of interests.

Authors' Contribution

H. Yan and H. Zhao participated in the design and coordination of the study, interpreted the data, and drafted and

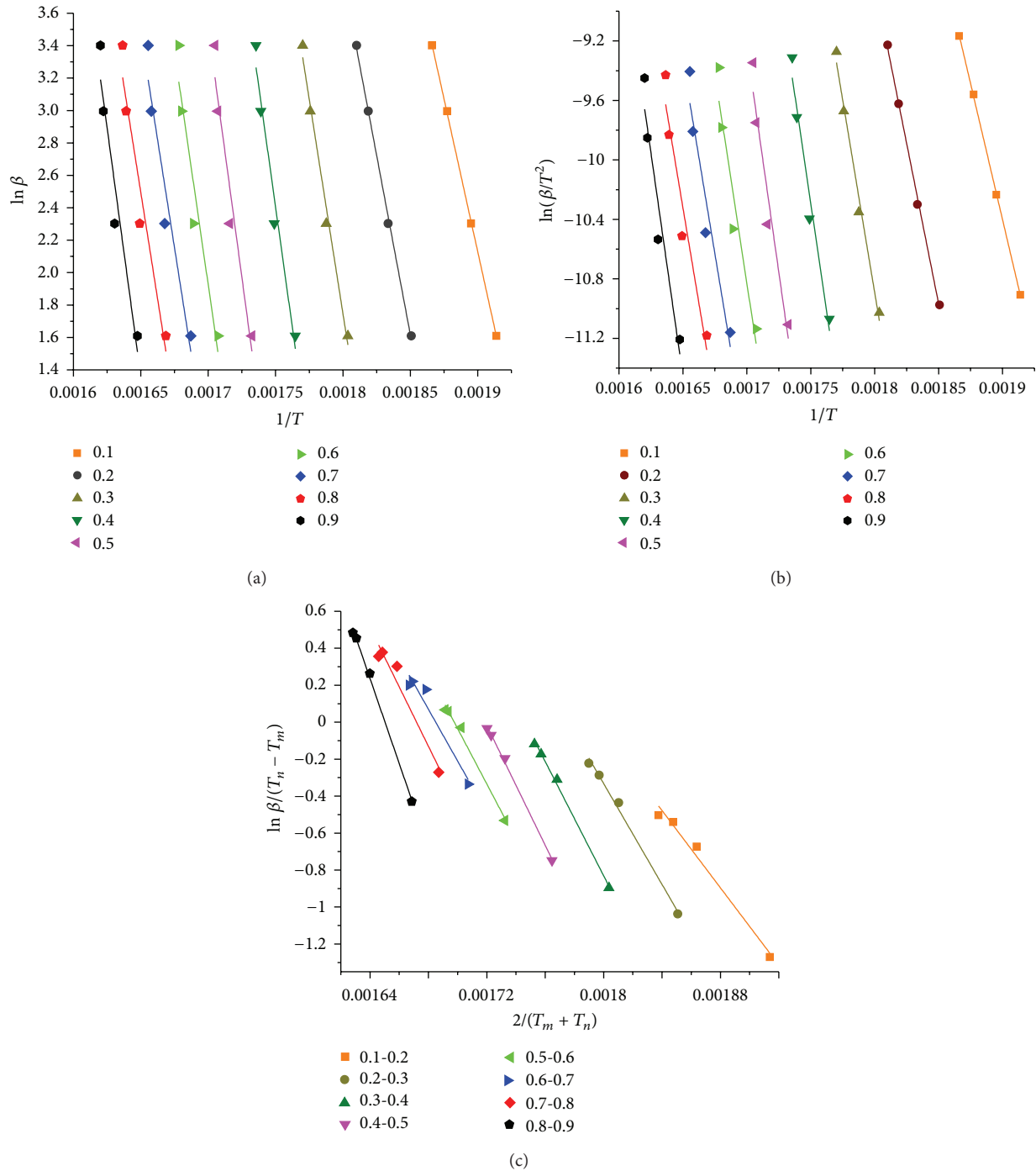


FIGURE 4: Plots for determining activation energy of Stage II of *H. annuus* stalk calculated by three methods ((a) FWO method; (b) KAS method; (c) Popescu method).

corrected the manuscript. Y. Zhang et al. participated in the interpretation of the data and corrected the draft paper. All authors read and approved the final paper.

Disclosure

H. Yan is a staff member of College of Chemical and Environmental Engineering, Shandong University of Science

and Technology, Qingdao, China. Dr. H. Zhao is the leader of Biochemical Engineering and Bioresources Laboratory at College of Chemical and Environmental Engineering. His areas of specialization are biochemical engineering, energy, and environmental engineering. He has published over 10 papers in international journals. Y. Zhang is one master degree candidate. Y. Tian and K. Xie are the leaders of Key Laboratory of Low-carbon Energy Chemical Engineering in

Universities of Shandong, Shandong University of Science and Technology, Qingdao 266590, China, and contributed to supply the excellent research platform and guide research works.

Acknowledgments

This work was financially supported by National Natural Science Foundation of China (21076117, 41202165), Open Funding from the State Key Laboratory of Crop Biology in Shandong Agricultural University (2010KF06 and 2011KF14), Projects of Shandong Province Higher Educational Science and Technology Program (J10LC15), Open Project Program of Key Lab of Marine Bioactive Substance and Modern Analytical Technique (MBSMAT-2012-03), and Qingdao Government Scientific and Technological Program.

References

- [1] T. Gollan, U. Schurr, and E. D. Schulze, "Stomatal response to drying soil in relation to changes in the xylem sap composition of *Helianthus annuus*. I. The concentration of cations, anions, amino acids in, and pH of, the xylem sap," *Plant, Cell & Environment*, vol. 15, no. 5, pp. 551–559, 1992.
- [2] H. Chen and T. Cutright, "EDTA and HEDTA effects on Cd, Cr, and Ni uptake by *Helianthus annuus*," *Chemosphere*, vol. 45, no. 1, pp. 21–28, 2001.
- [3] S. Yorgun, S. Şensöza, and O. M. Koçkar, "Flash pyrolysis of sunflower oil cake for production of liquid fuels," *Journal of Analytical and Applied Pyrolysis*, vol. 60, no. 1, pp. 1–12, 2001.
- [4] J. M. Encinar, F. J. Beltrán, J. F. González, and M. J. Moreno, "Pyrolysis of maize, sunflower, grape and tobacco residues," *Journal of Chemical Technology and Biotechnology*, vol. 70, no. 4, pp. 400–410, 1997.
- [5] P. Pan, C. Hu, W. Yang et al., "The direct pyrolysis and catalytic pyrolysis of *Nannochloropsis* sp. residue for renewable bio-oils," *Bioresource Technology*, vol. 101, no. 12, pp. 4593–4599, 2010.
- [6] Y. Tonbul, A. Saydut, K. Yurdakoç, and C. Hamamcı, "A kinetic investigation on the pyrolysis of *Seguruk asphaltite*," *Journal of Thermal Analysis and Calorimetry*, vol. 95, no. 1, pp. 197–202, 2009.
- [7] A. Szydłowska-Czerniak, K. Trokowski, and E. Szlyk, "Optimization of extraction conditions of antioxidants from sunflower shells (*Helianthus annuus* L.) before and after enzymatic treatment," *Industrial Crops and Products*, vol. 33, no. 1, pp. 123–131, 2011.
- [8] A. E. Pütün, A. Özcan, H. F. Gerçel, and E. Pütün, "Production of biocrudes from biomass in a fixed-bed tubular reactor: product yields and compositions," *Fuel*, vol. 80, no. 10, pp. 1371–1378, 2001.
- [9] H. R. Yuan, R. H. Liu, H. Jiang, and Y. Y. Hao, "Kinetic study of sunflower seed husk pyrolysis," *Transactions of the Chinese Society of Agricultural Engineering*, vol. 22, no. 4, pp. 220–223, 2006.
- [10] M. Carrier, A. Loppinet-Serani, D. Denux et al., "Thermogravimetric analysis as a new method to determine the lignocellulosic composition of biomass," *Biomass and Bioenergy*, vol. 35, no. 1, pp. 298–307, 2011.
- [11] R. French and S. Czernik, "Catalytic pyrolysis of biomass for biofuels production," *Fuel Processing Technology*, vol. 91, no. 1, pp. 25–32, 2010.
- [12] H. Zhao, H. Yan, S. Dong et al., "Thermogravimetry study of the pyrolytic characteristics and kinetics of macro-algae *Macrocystis pyrifera* residue," *Journal of Thermal Analysis and Calorimetry*, 2011.
- [13] H. Zhao, H. Yan, C. Zhang et al., "Pyrolytic characteristics and kinetics of phragmites australis," *Evidence-Based Complementary and Alternative Medicine*, vol. 2011, Article ID 408973, 6 pages, 2011.
- [14] J. Guo and A. C. Lua, "Kinetic study on pyrolysis of extracted oil palm fiber. Isothermal and non-isothermal conditions," *Journal of Thermal Analysis and Calorimetry*, vol. 59, no. 3, pp. 763–774, 2000.
- [15] S. Xiu, H. K. Rojanala, A. Shahbazi, E. H. Fini, and L. Wang, "Pyrolysis and combustion characteristics of Bio-oil from swine manure," *Journal of Thermal Analysis and Calorimetry*, vol. 107, pp. 823–829, 2012.
- [16] H. Zhao, H. Yan, M. Liu, C. Zhang, and S. Qin, "Pyrolytic characteristics and kinetics of the marine green tide macroalgae, *Enteromorpha prolifera*," *Chinese Journal of Oceanology and Limnology*, vol. 29, no. 5, pp. 996–1001, 2011.
- [17] A. Ji, S. Zhang, X. Lu, and Y. Liu, "A new method for evaluating the sewage sludge pyrolysis kinetics," *Waste Management*, vol. 30, no. 7, pp. 1225–1229, 2010.
- [18] J. H. Flynn and L. A. Wall, "A quick direct method for determination of activation energy from thermogravimetric data," *Journal of Polymer Science B*, vol. 4, pp. 423–428, 1966.
- [19] M. S. Subramanian, R. N. Singh, and H. D. Sharma, "Reaction kinetics of some actinide oxalates by differential thermal analysis," *Journal of Inorganic and Nuclear Chemistry*, vol. 31, no. 12, pp. 3789–3795, 1969.
- [20] A. Aboulkas, K. El Harfi, A. El Bouadili, and M. Nadifiyine, "Study on the pyrolysis of Moroccan oil shale with poly (ethylene terephthalate)," *Journal of Thermal Analysis and Calorimetry*, vol. 100, no. 1, pp. 323–330, 2010.
- [21] D. Li, L. Chen, J. Zhao et al., "Evaluation of the pyrolytic and kinetic characteristics of *Enteromorpha prolifera* as a source of renewable bio-fuel from the Yellow Sea of China," *Chemical Engineering Research and Design*, vol. 88, no. 5–6, pp. 647–652, 2010.
- [22] W. Peng, Q. Wu, P. Tu, and N. Zhao, "Pyrolytic characteristics of microalgae as renewable energy source determined by thermogravimetric analysis," *Bioresource Technology*, vol. 80, no. 1, pp. 1–7, 2001.
- [23] J. M. Cai and L. S. Bi, "Kinetic analysis of wheat straw pyrolysis using isoconversional methods," *Journal of Thermal Analysis and Calorimetry*, vol. 98, no. 1, pp. 325–330, 2009.
- [24] A. A. Zabaniotou, E. K. Kantarelis, and D. C. Theodoropoulos, "Sunflower shells utilization for energetic purposes in an integrated approach of energy crops: laboratory study pyrolysis and kinetics," *Bioresource Technology*, vol. 99, no. 8, pp. 3174–3181, 2008.
- [25] A. Sharma and T. R. Rao, "Kinetics of pyrolysis of rice husk," *Bioresource Technology*, vol. 67, no. 1, pp. 53–59, 1999.
- [26] T. A. Ngo, J. Kim, and S. S. Kim, "Characteristics and kinetics of cattle litter pyrolysis in a tubing reactor," *Bioresource Technology*, vol. 101, no. 1, supplement, pp. S104–S108, 2010.
- [27] R. Z. Hu, S. L. Gao, F. Q. Zhao et al., *Thermal Analysis Kinetics*, Science Press, Beijing, China, 2nd edition, 2008.
- [28] Z. Shuping, W. Yulong, Y. Mingde, L. Chun, and T. Junmao, "Pyrolysis characteristics and kinetics of the marine microalgae *Dunaliella tertiolecta* using thermogravimetric analyzer," *Bioresource Technology*, vol. 101, no. 1, pp. 359–365, 2010.

- [29] M. Jefferson, "Sustainable energy development: performance and prospects," *Renewable Energy*, vol. 31, no. 5, pp. 571-582, 2006.



Hindawi

Submit your manuscripts at
<http://www.hindawi.com>

